Computers in Biology and Medicine 150 (2022) 106144

Contents lists available at ScienceDirect

Computers in Biology and Medicine

journal homepage: www.elsevier.com/locate/compbiomed

ComEDA: A new tool for stress assessment based on electrodermal activity

Mimma Nardelli [a,*], Alberto Greco [a], Laura Sebastiani [b], Enzo Pasquale Scilingo [a]

[a] Bioengineering and Robotics Research Centre E. Piaggio and Dipartimento di Ingegneria dell'Informazione, University of Pisa, Largo Lucio Lazzarino 1, Pisa, 56122, Italy

[b] Department of Translational Research and New Technologies in Medicine and Surgery, University of Pisa, via Paolo Savi 10, Pisa, 56126, Italy

ARTICLE INFO

Keywords:
Electrodermal activity (EDA)
Skin conductance
Stress
Arousal
Complexity
Phase space reconstruction

ABSTRACT

Non-specific sympathetic arousal responses to different stressful elicitations can be easily recognized from the analysis of physiological signals. However, neural patterns of sympathetic arousal during physical and mental fatigue are clearly not unitary. In the context of physiological monitoring through wearable and non-invasive devices, electrodermal activity (EDA) is the most effective and widely used marker of sympathetic activation. This study presents ComEDA, a novel approach for the characterization of complex dynamics of EDA. ComEDA overcomes the methodological limitations related to the application of nonlinear analysis to EDA dynamics, is not parameter-sensitive and is suitable for the analysis of ultra-short time series. We validated the proposed algorithm using synthetic series of white noise and 1/f noise, varying the number of samples from 50 to 5000. By applying our approach, we were able to discriminate a statistically significant increase of complexity in the 1/f noise with respect to white noise, obtaining p-values in the range [4.35×10^{-6}, 0.03] after the Mann–Whitney test. Then, we tested ComEDA on both EDA signal and its tonic and phasic components, acquired from healthy subjects during four experimental protocols: two inducing a sympathetic activation through physical efforts and two based on mentally stressful tasks. Results are encouraging and promising, outperforming state of the art metrics such as the Sample Entropy. ComEDA shows good performance not only in discriminating between stressful tasks and resting state (p-value < 0.01 after the Wilcoxon non-parametric statistical test applied to EDA signals of all the four datasets), but also in differentiating different trends of complexity of EDA dynamics when induced by physical and mental stressors. These findings suggest future applications to automatically detect and selectively identify threats due to overwhelming stress impacting both physical and mental health or in the field of telemedicine to monitor autonomic diseases correlated to atypical sympathetic activation. The Matlab code implementing the ComEDA algorithm is available online.

1. Introduction

Electrodermal activity (EDA) is a general term that reflects any variation in the bioelectric properties of the skin. These alterations are caused by the activity of eccrine sweat glands, which is regulated by the sympathetic nervous system, through the sudomotor innervation [1,2]. EDA signals can be divided into two main components: a tonic component, which incorporates the baseline slow drifts and spontaneous fluctuations (skin conductance level, SCL), and the phasic component, that depicts the short-term fast-varying response to external stimuli (skin conductance response, SCR) [3]. In contrast to other autonomic nervous systems (ANS) correlates, e.g., heart rate variability (HRV), EDA is solely controlled by the sympathetic nervous system and can be considered a pure arousal indicator [4–6].

ANS dynamics are intrinsically complex and the interplay between autonomic sub-systems is characterized by nonlinear relationships [7–9]. For this reason, the chaos theory represents an effective complementary tool to unveil hidden information of the ANS. For instance, the nonlinear analysis of HRV and blood pressure time series [10,11] has provided relevant results in distinguishing emotional and cognitive responses [12–14].

On the other hand, only a few studies have investigated the complexity of the EDA signals. During a sympathetic activation, the EDA dynamics response is characterized by a sequence of rapid spiky increases, followed by a slower exponential decay back to baseline [3,15–17]. This peculiar dynamics has limited the application of many nonlinear analysis methods, e.g. entropy algorithms, because their approach, based on the study of similarities of phase space vectors, results to be less accurate when the mean and the standard deviation of the time series show remarkable fluctuations [18,19]. Among the few

* Corresponding author.
E-mail address: mimma.nardelli@unipi.it (M. Nardelli).

https://doi.org/10.1016/j.compbiomed.2022.106144
Received 19 April 2022; Received in revised form 15 September 2022; Accepted 24 September 2022
Available online 30 September 2022

previous studies, the application of symbolic information and approximate entropy to EDA has highlighted a more task-specific response of nonlinear theory indexes to mental cognitive stressors, with respect to traditional time-domain features, as the electrodermal response amplitude [20]. Svetlak et al. suggested that complexity analysis can be more sensitive to the huge amount of functional and spatial mechanisms influencing EDA modulation from various areas of the brain during mental efforts [21].

In this study, we use chaos theory to investigate the complexity of EDA dynamics, to overcome the limitations of standard analysis in the time and frequency domain, which has been demonstrated to distinguish different arousal levels, but is unable to identify different kinds of stressful elicitations. In fact, the sympathetic activation can be related to a wide range of stressor conditions, which go from physical efforts [22–24], to stressful mental tasks [25–27]. A comparison between EDA responses to physical and cognitive stressors using different acquisition systems and sites, has been reported in [28]. In all the experiments, EDA gradually decreased to a plateau during the baseline recorded in resting-state condition, and increased during the arousing tasks, presenting multiple electrodermal responses during the whole task duration. Considering EDA quantifiers in time and frequency domains, statistically significant differences between resting state and stressful tasks were reported in [29]. However, the traditional analysis of the EDA signal during stressful tasks, while effectively recognizing the arousal rise related to stress, does not allow the correct identification of its origin, whether physical or cognitive, since the values of the parameters follow the same trend. In that study, in fact, an increase of the skin conductance level was found during orthostatic, physical, and cognitive stress protocols. In all three experimental protocols, a consistent increment in the values of EDAsymp, a new estimator of sympathetic activity based on the power spectral density of EDA, was also identified.

Although different tasks often induce a similar response in the EDA time series, neural patterns of sympathetic arousal responses following physical efforts or mental stressors are clearly not unitary [30]. Hippocampus, amygdala, and prefrontal cortex play a crucial role in cortisol regulation in response to mental stressors, whereas the brainstem, the nucleus of the solitary tract, and the ventrolateral medulla are mainly involved during physical fatigue [31–33]. The central regulation of EDA dynamics is characterized by numerous and complex regulatory mechanisms and different neural pathways. Indeed, previous studies have hypothesized that EDA changes could be influenced by different independent pathways originated at cortical (premotor cortex and pyramidal pathways) or subcortical levels (hypothalamus and amygdala) [3,20,34]. Moreover, another EDA regulation center has been identified in the reticular formation localized to the brainstem [34].

We propose here ComEDA, an *ad-hoc* algorithm based on the reconstruction of EDA dynamics in the phase-space. Our method overcomes the issues related to the typical amplitude fluctuations of the EDA signal, by computing the angular distances of the points in the phase space to analyze the trajectories of the EDA attractor. This approach of complexity analysis has been already applied to other physiological signals with similar characteristics, e.g. electrohysterogram [35], with satisfactory and promising results. Once the attractor is successfully reconstructed we quantify its spacial complexity using the normalized quadratic Rényi entropy of the probability density function (PDF) of such distances, computed through a kernel density estimation technique. Our approach is designed for a reliable analysis of ultra-short EDA time-series, in order to capture the complex dynamics of the fast EDA response to stressful tasks. Furthermore, it is worthwhile noting that we do not resort to pre-set parameters that can lead to unspecific results, but each parameter used in the algorithm is computed according to the input time series.

We tested our method on four different datasets of EDA signals acquired from healthy subjects during four experiments, two protocols structured to induce physical effort and two protocols based on stressful mental tasks. Specifically, we analyzed the complexity of EDA dynamics during a hand-grip task, performed at the submaximal voluntary contraction, a forced maximal exhalation protocol, a mental computation task, and a Stroop Color and Word test. For each task, we applied the ComEDA algorithm on the physiological signals acquired during each task compared to the preceding resting-state condition, considering three different input time series: the EDA signal and the two main signals into which it can be decomposed, i.e. tonic and phasic, extracted by using the cvxEDA approach [17]. Performance of ComEDA were compared with state of the art Sample Entropy (SampEn) [19,36].

Experimental results demonstrate that the novel ComEDA approach proposed here is able to distinguish different changes in complex dynamics of EDA time series, reflecting the two typologies of stressful stimuli, i.e. physical efforts and mental fatigue.

2. Materials and methods

We tested ComEDA algorithm as a method to quantify complexity of dynamical systems by using both synthetic time series and physiological signals. In Section 2.1 we describe data simulation, whereas in Section 2.2.1 the details about the four experimental protocols used to acquire EDA signals are reported. The pre-processing of EDA signals by using cvxEDA, and the complexity analysis follow in Sections 2.3 and 2.2.2. Fig. 1 shows the overall scheme of the experimental design we followed in this study to acquire and process real data.

2.1. Synthetic series

We first tested the ComEDA algorithm on simulated series of white gaussian noise (WGN) and 1/f noise, as reported in previous scientific literature on complexity indexes [37–39]. We simulated 200 realizations of WGN and 200 realizations of 1/f series of 5000 samples, and we applied the ComEDA method to discriminate the corresponding complexity level by using windows of different sizes in the range [50, 5000] samples, with intervals of 300 samples. We compared the complexity degree referred to the two processes by using the statistical analyses described in Section 2.4.

2.2. Physiological data

2.2.1. Data acquisition

In this study we designed and conducted four different experimental protocols based on stressful stimuli (see Fig. 1(a)). The first two experiments (Exp1 and Exp2) are centered on physical stressful tasks, i.e. submaximal hand-grip and forced maximal exhalation tasks. Exp3 and Exp4 are based on two stress-inducing tasks: mental computation task and the Stroop Color and Word test, respectively. The selection of the specific stressful tasks used in this study is based on the results obtained in previous scientific literature on the analysis of sympathetic response evoked by physical or mental stimuli [24,40–42]. The experimental protocols, the criteria adopted for subject recruitment and processing of personal data were approved by the "Bioethics Committee of the University of Pisa" (protocol n. 3/2019). According to the self-report questionnaires filled before the four experiments, none of the participants suffered from any cardiovascular, mental or sweat-related diseases (e.g. hyperhidrosis). The details of all the experimental protocols follow below.

Submaximal hand-grip protocol (Exp1)

In this experiment (Exp1), 27 healthy subjects (aged 22–41, mean age: 28.64, 13 males) provided their written informed consent to participate. During the experiment, participants were asked to stay seated with their eyes open. The experimental protocol consisted in one resting-state session of one-minute and one-minute of isometric hand-grip performed at 33% of maximal voluntary contraction (task *hg*). The hand-grip was executed by using a hand dynamometer, and the maximal hand-grip force was calculated as the highest value among

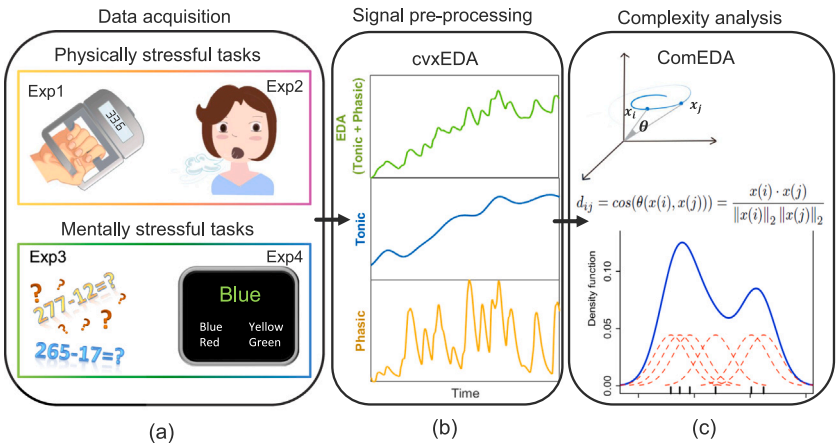

Fig. 1. Overall experimental design of the study. (a) EDA signals were acquired during four different experimental protocols (see details in Section 2.2.1): two based on stress induced by physical efforts (Exp1 and Exp2) and two based on stress induced by mental/cognitive tasks (Exp3 and Exp4). (b) Signal pre-processing block shows the application of cvxEDA algorithm (see Section 2.2.2). After applying cvxEDA, three time series can be derived from each EDA signal: noise-free EDA signal and its two embodied components (tonic and phasic). The plots represent the three time series derived from one EDA signal by using cvxEDA. (c) The novel ComEDA algorithm was applied to each of the three time series resulting from cvxEDA-based pre-processing, in order to assess changes in the complexity level of physiological dynamics, according to the stressful tasks of the four experimental protocol. The angular distance between two points of the trajectory in a representative phase space is shown with the related formula, together with an example of a probability density function used to study the distance distribution in the ComEDA algorithm (see Section 2.3.1).

three trials of a 3-s maximal effort performed before starting the experiment. The BIOPAC MP150 system was used to acquire the EDA signals from the fingers of non-dominant hand of each participant, with sampling rate of 500 Hz.

Forced maximal exhalation protocol (Exp2)

In this experiment (Exp2), 16 healthy subjects (aged 18–35) were recruited. Before taking part in the study, each subject gave a written informed consent. Participants were asked to perform a forced maximal exhalation task, breathing out with the utmost intensity [24]. The protocol started with a 3-min session where the subjects began breathing normally and resting in front of a gray monitor. Thereafter, the participants were asked to perform a deep exhalation each time the background color of the screen changed to black (*resp* task). There were three stimulation sessions in which participants had to perform a deep exhalation each time the background color of the screen changed to black (*resp* task). Three sessions were planned and in each one the participants should deeply exhale six times with a variable interstimulus interval, randomly selected among 4, 8, and 12 s. A 30-s recovery interval was used to separate consecutive experimental sessions. During the whole duration of the experiment, EDA signals and the respiration efforts were acquired by using a Biosemi Active II system.

This experimental paradigm is intended to induce a sympathetic activation through an objective and reliable procedure, unaffected by emotional components. According to the literature, EDA signals acquired during such tasks, exhibit more stable waveform patterns and less habituation than other means of elicitation, e.g. electrical stimulation [24].

Mental computation protocol (Exp3)

The third experiment (Exp3) recruited 24 participants (aged 22–26) who gave their informed consent to take part in the study. After a closed-eyes resting state session of two minutes at the beginning of the experimental protocol, the volunteers were asked to perform a mental computation task (*mc* task). Specifically, they were asked to subtract alternately 12 and 17 starting from 277, down to a 2-digit number, then multiply the obtained number by two and finally start over the series of subtractions. In case of error, the participant had to start the calculation over. During the whole duration of the experiment, the BIOPAC MP150 system was used to acquire the EDA signals from the fingers of non-dominant hand.

Stroop Color and Word Test (Exp4)

The fourth experiment (Exp4) involved 31 healthy subjects (aged 21–50). Participants underwent the Stroop Color and Word Test, a well-known neuropsychological test used to assess the ability to inhibit cognitive interference generated when the processing of a specific stimulus feature curbs the simultaneous processing of a second stimulus attribute [43,44]. Subjects gave their informed consent and the experiment started with five minutes of open-eyes resting state session. In the Stroop Color and Word Test color-words were printed in an inconsistent color ink (for instance the word 'yellow' was printed in red ink) and displayed on a black computer screen every 2 s. A palette of four colors was used: yellow, red, blue, and green. In this stressful task, lasting overall three minutes, the participants were asked to click on the right color (and not on the meaning) of the presented words, choosing among the four colors written in white on the bottom of the screen. At the top of the screen a counter showed the number of correct answers and it was reset to zero on each error. EDA signals were recorded from non-dominant hand of each participant by using the Shimmer 3 GSR+ device.

2.2.2. EDA signal pre-processing: cvxEDA

The cvxEDA algorithm was applied as pre-processing step to remove artifacts from each EDA signal and at the same time to extract its main components: the tonic and the phasic components. In fact, cvxEDA models the skin conductance as the sum of the tonic and phasic signals plus an additive noise term representing modeling and measurement errors [17]. The tonic component presents slow and spontaneous fluctuations of the baseline level. On the other hand, the phasic component represents fast-varying superimposed skin conductance changes directly evoked by the stimulus. After the application of cvxEDA, we obtained from each EDA time series its phasic and tonic components (see the example plots in Fig. 1(b)). As already mentioned, for a full characterization of complex dynamics underlying skin conductance, we applied the ComEDA algorithm not only to the cleaned EDA time series (given by the sum of the tonic and phasic signals), but also to the two related components, i.e., the tonic and phasic components, which have different time-scale and relationship to the triggering stimuli [3]. Before applying ComEDA, each time series was rescaled using a min–max normalization, shifting the minimum and maximum amplitude values to 0 and 1. Since the EDA signal bandwidth remains below 2 Hz [45], a frequency rate of 4 Hz was used for all the time series in this study. This sampling rate is also the one used by many wearable devices on the market for continuous monitoring of skin conductance.

2.3. Complexity analysis

As mentioned above, for each acquisition, three signals were considered: the tonic and phasic components obtained after the application of cvxEDA algorithm, and their sum, which represents the EDA signal without noise components (hereinafter EDA).

We applied the here proposed algorithm for the complexity assessment of skin conductance dynamics, i.e., ComEDA, together with the gold standard of the entropy measures introduced for the study of physiological time series, i.e., SampEn [19,46]. The details on the computation of ComEDA algorithm are reported in Section 2.3.1 and the SampEn method is described in Section 2.3.2.

2.3.1. ComEDA algorithm

The here proposed ComEDA approach aims at characterizing the spatial complexity of nonlinear EDA dynamics in the phase space. The following steps are designed to achieve that objective:

1. Phase space reconstruction;
2. Calculation of the angular distances between all the pairs of points in the phase space;
3. Computation of the probability density function (PDF) of the distances;
4. Quadratic Rényi entropy of the PDF.

(1) Phase space reconstruction: The first step of the ComEDA algorithm is the reconstruction of the attractor related to each time series (EDA signal, tonic and phasic components) in its own phase space, by using the Takens' time-delay embedding method [47]. For each time series, the embedding dimension m (the number of the phase space coordinates) is computed by using the False Nearest Neighbors (FNN) procedure [48]. The embedding vectors in the new space consist in vectors of delayed values of the time series considered, where the optimal time delay τ is calculated as the first minimum of the auto-mutual information function [49]. Once the values of m and τ are calculated for a given time series $[x(1), x(2), \dots, x(N)]$ (that can be either EDA, phasic or tonic time series) of length N, a total number of $n = N-(m-1)\tau$ embedding vectors are defined as follows:

$$X(k) = [x(k), x(k-\tau), x(k-2\tau), \dots, x(k-(m-1)\tau)] \quad (1)$$

(2) Calculation of the angular distances: The distance d_{ij} between two phase space vectors $X(i)$ and $X(j)$, for all $1 \le i, j \le n = N-(m-1)\tau$, is defined observing the angle between them [35], as follows:

$$d_{ij} = cos(\theta(X(i), X(j))) = \frac{X(i) \cdot X(j)}{\|X(i)\|_2 \, \|X(j)\|_2} \quad (2)$$

where $\cdot$ represents the inner product and $\|\|_2$ is the Euclidean norm. The total number of d_{ij} values is $n(n-1)/2$, without considering self-matches (d_{ii}) and given that $d_{ji} = d_{ij}$.

(3) Computation of the probability density function (PDF): To limit the parameter dependence, we did not use a threshold value to compare the distances. We globally quantify the spatial distribution of the trajectory points in the phase space, using an approach inspired to distribution entropy algorithm, where the histogram of the distance values was analyzed [50,51]. In ComEDA, the PDF related to the values of angular distances d_{ij} is computed by using a kernel density estimator based on linear diffusion processes [52], with a Gaussian kernel. The number of bins B of the PDF is chosen applying the Sturges method [53].

(4) Quadratic Rényi entropy of the PDF: After computing the probability of each bin (p_i), the quadratic Rényi entropy formula is applied [54]:

$$H_2 = -log_2\left(\sum_{i=1}^{B} p_i^2\right) \quad (3)$$

The value obtained is then normalized to the range [0,1], as follows:

$$ComEDA = -\frac{1}{log_2 B} H_2 \quad (4)$$

As it can be noticed, ComEDA algorithm does not need to set any a priori parameters, unlike the other algorithms in the literature. All the parameters used in the ComEDA algorithm are selected in order to be the optimal metrics for each specific time series used as input. The normalization procedure allows simpler comparisons between the results obtained under different experimental conditions.

2.3.2. SampEn algorithm

Concerning the computation of SampEn approach, we considered the same phase space reconstruction we described in Section 2.3.1. Regarding the choice of the parameters m and τ, we considered the same values used for ComEDA, obtained applying the FNN procedure and the auto-mutual information function for each time series.

Then, we applied the procedure described in [19,46].

Considering each pair of vectors $X(i)$ and $X(j)$ in the phase space, their Chebyshev distance $d_{ij} = max_c|x(i+c\tau) - x(j+c\tau)|$ (with $0 \le c \le m-1$) was computed excluding self-matches ($i = j$). Then we estimated the value of $C^m(r)$, i.e. the probability that two vectors $X(i)$ and $X(j)$ of m coordinates will match, as follows:

$$C^m(r) = \frac{1}{N-m}\sum_{i=1}^{N-m}\left(\frac{1}{N-m-1}\sum_{i=1, i\neq j}^{N-m}\mathcal{H}(r-d_{i,j})\right) \quad (5)$$

where $\mathcal{H}$ is the Heaviside function. The parameter r is the threshold used to compare the distance values between the vectors, and is usually chosen between 10%–25% of the time series standard deviation [55]. In this study, we set r equal to the 25% of the standard deviation of the studied series, i.e. EDA, tonic or phasic components [20]. The embedding dimension was then increased from m to $m+1$, and $C^{m+1}(r)$ was calculated. Finally, the SampEn value was found as the negative natural logarithm of the conditional probability that two sequences similar for m points remain similar for $m+1$ points (without self-comparisons), as follows:

$$\text{SampEn(m,r,N)} = -\ln\frac{C^{m+1}}{C^m} \quad (6)$$

2.3.3. Comparison between ComEDA and previous entropy algorithms

The ComEDA approach aims to overcome some critical limitations of existing entropy algorithms [18,19,56] used to quantitatively describe the evolution of a dynamical system through the characterization of the distances of the points constituting the attractor within the reconstructed phase space. The way of quantifying the dispersion of trajectory points is made radically different in ComEDA, compared to previous methods. The first main difference is the computation of the distance between each pair of points along the trajectory in the phase space.

Traditional entropy metrics investigate the similarity of each pair of phase space vectors, e.g. $X(i)$ and $X(j)$, by computing the Chebyshev distance. Such a distance is usually compared with a threshold value, depending on the standard deviation of the time-series (usually the 15%–20% of the standard deviation [46]). However, this standard approach cannot be easily applied to the EDA and phasic signals due to their spiky nature. To overcome this limitation, ComEDA algorithm is based on a modified computation of distance metrics, based on angular distance (see Eq. (2)).

In ComEDA, also the way to compare the values of the distances between the vectors is different, since it is based on the kernel density estimation of the PDF of the distance values. The analysis of the PDF makes the ComEDA algorithm free from the choice of the threshold value and is based on the whole information coming from all the pairs of points and not only from those with a distance below the threshold, such as in SampEn for example.

Finally, the calculation of the Rényi entropy allows to characterize the entropy from the PDF, giving a global measure of the spatial distribution of the points in the phase space, without the need to study their behavior as the embedding distance varies.

2.4. Statistical analysis

Concerning the results of the application of ComEDA approach on synthetic series, we compared the median values of the complexity levels by applying the Mann–Whitney non-parametric test for unpaired samples [57]. We used non-parametric tests given the non-gaussian distribution of samples, as demonstrated by the application of Shapiro–Wilk test, which is considered the most powerful normality test for all types of distribution and sample sizes [58]. We obtained a p-value for each comparison between 200 WGN series and 200 1/f series varying the number of samples from 50 to 5000 (considering an interval of 300 samples each time). The false discovery rate (FDR) adjustment through the Benjamini–Yekutieli correction [59] was applied on the 17 p-values obtained.

Considering each experimental protocol separately, we extracted one value of ComEDA (or SampEn) for each session, obtaining two vectors of length equal to the number of subjects to be compared, one related to the stressful task and the other related to the resting state. Before testing the statistical differences between the ComEDA (or SampEn) values extracted from the EDA, tonic, and phasic signals during the stressful and rest sessions of the four protocols, we verified the non-gaussianity of the sample distributions using the Shapiro–Wilk test. Once the non-gaussianity of the distributions of ComEDA values was verified (p-value < 0.05 after Shapiro–Wilk test), we used a two-tailed Wilcoxon signed-rank test to compare resting state sessions and stressful tasks, which is a non-parametric statistical test for matched-pair data [60]. The same statistical tests were applied to SampEn values, in order to compare the performance of the two different algorithms. Also in the case of real data, we used the FDR approach as *post-hoc* statistical analysis, considering all the twelve p-values obtained after the Wilcoxon tests for both ComEDA and SampEn (all the comparisons reported in Tables 1 and 2 respectively).

3. Results

3.1. Synthetic series

Applying ComEDA approach to discriminate WGN and 1/f series, we were able to identify pink noise series as the most complex. After the Mann–Whitney non-parametric tests and the FDR adjustment through the Benjamini–Yekutieli correction, we obtained a significant p-value ($p < 0.05$) for all the 17 comparisons, considering different window sizes. Specifically, the p-values were in the range $[4.35 \times 10^{-6}, 0.03]$, and for each duration the ComEDA median value related to 1/f noise was higher than the median value obtained for WGN series.

In Figs. 2 and 3 we reported the boxplots of the ComEDA values for WGN and 1/f noise for series with a duration lower and higher than 1200 samples, respectively. Considering that we used physiological series sampled at 4 Hz, the window dimension of 1200 samples corresponds to series of 5 min in the real case, which is the threshold below which time series are considered ultra-short [13]. Observing each couple of boxplots (WGN and 1/f series) related to each value of length considered, it can easily be noticed that the median value of comEDA indexes referred to 1/f noise is higher than the median value referred to WGN noise.

3.2. Physiological data

In this section, we report the results of the statistical analysis applied to the ComEDA and SampEn estimates related to the four datasets.

Table 1 shows the p-values obtained after the application Wilcoxon statistical test to the paired ComEDA values computed from EDA signals both during the stressful tasks and the previous resting state, and then corrected through the FDR multiple-comparisons procedure. Specifically, ComEDA has been evaluated from all of the three types of signal: EDA, tonic and phasic time series. For each signal and for each experimental protocol we reported the p-value of the Wilcoxon test and the trend of the median values of complexity estimates going from the resting state to the stressful tasks.

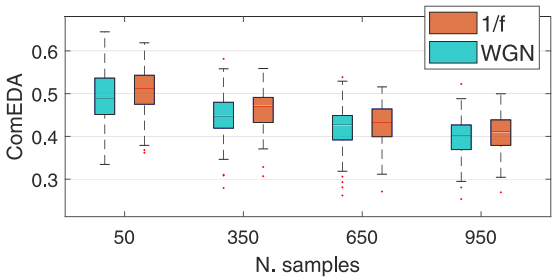

Fig. 2. Boxplots of ComEDA values obtained from 200 realizations of WGN and 1/f series, considering ultra-short windows with increasing number of samples from 50 to 950. In correspondence with each value on the horizontal axis concerning the length of the synthetic series considered, two boxplots have been reported that provide a visualization of summary statistics for the ComEDA values extracted from white noise (WGN) and 1/f noise, respectively. The distance between the bottom and top of each colored box represents the interquartile range. The middle line in each box is the median value.

Table 1
Results of statistical tests applied to ComEDA values extracted from EDA, tonic and phasic time series in the four experimental protocols used in this study (Exp1, Exp2, Exp3, Exp4), in terms of p-values obtained from the application of Wilcoxon non-parametric test, and corrected through FDR procedure. For each test, the corresponding trend of ComEDA median value is shown by using the symbols ↓ and ↑, which indicate a decrease and an increase of ComEDA median values during the stressful task with respect to the preceding rest, respectively. *n.s.* stands for not-significant p-value (p-value > 0.05).

	ComEDA					
	EDA		Tonic		Phasic	
	p-value	Trend	p-value	Trend	p-value	Trend
Exp1 (rest vs. hg)	0.0088	↓	0.0411	↓	n. s.	
Exp2 (rest vs. resp)	0.0032	↓	0.0052	↓	0.0299	↓
Exp3 (rest vs. mc)	0.0043	↑	n.s.		0.0011	↓
Exp4 (rest vs. stroop)	0.0003	↑	0.0242	↑	n.s.	

It can be easily noticed that ComEDA algorithm applied to EDA signals gave significantly different values when resting and stressful sessions were compared, in all the experiments. Fig. 4 shows the results obtained applying ComEDA algorithm to EDA signals acquired during all the four experimental protocols in terms of violin plots [61], that combine the data density traces and the box plots. Two specular trends of median ComEDA values were identified comparing the results of the first two protocols based on carrying out stressful physical tasks and the last two experiments which aimed at increasing mental workload. We found a significant decrease of complexity in EDA signals during the first two experimental protocols: hand-grip (*hg* in Exp1) and forced maximal exhalation (*resp* in Exp2) tasks. In other words, EDA showed lower complexity during the physical stressors than during the previous resting state (p-value < 0.01). On the other hand, ComEDA values increased when subjects performed mental computation task (*mc* in Exp3, p-value < 0.01) and the Stroop test in Exp4 (p-value < 0.001).

For the sake of completeness, in the Table 1 we also report the ComEDA figures calculated on the tonic and phasic components, although some values resulted to be not statistically significant (see *n.s.* notation in the Table). In summary, the ComEDA estimates from tonic components decreased during the physical effort tasks in Exp1 (p-value < 0.05), Exp2 (p-value < 0.01) and increased during the cognitive effort

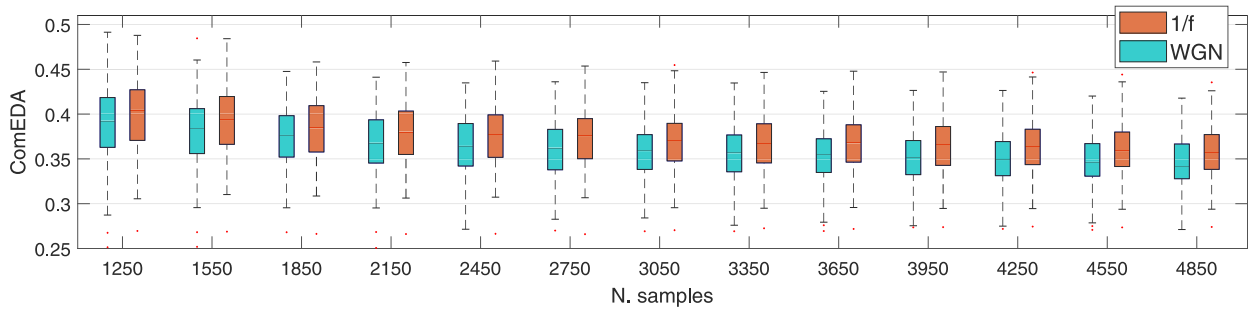

Fig. 3. Boxplots of ComEDA values obtained from 200 realizations of WGN and 1/f series, considering windows with increasing number of samples from 1250 to 4850. In correspondence with each value on the horizontal axis concerning the length of the synthetic series considered, two boxplots have been reported that provide a visualization of summary statistics for the ComEDA values extracted from white noise (WGN) and 1/f noise, respectively. The distance between the bottom and top of each colored box represents the interquartile range. The middle line in each box is the median value.

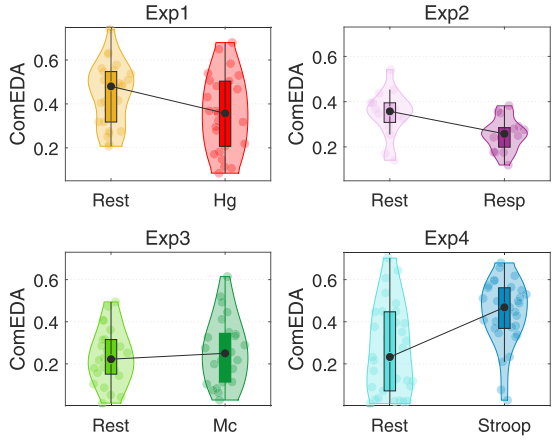

Fig. 4. Violin plots of ComEDA vales obtained from EDA signals related to arousal tasks of Exp1, Exp2, Exp3, and Exp4, compared to the corresponding previous resting state session. Each Violin plot combines the box plot with the density traces of the related data plotted symmetrically ro the left anf the right of the box plot. The points shown between the two density curves of each violin plot illustrate the individual ComEDA values according to each experimental condition. The black straight line highlights the trend of ComEDA median values.

in Exp4 (p-value < 0.05). Consistently with the EDA signals, an increase in the median values of ComEDA was found also during the *mc* task in Exp3, even if the result of statistical test was not significant (p-value > 0.05).

Looking at the results of ComEDA from phasic components the only statistically significant results have been achieved for the tasks *resp* in Exp2 and *mc* in Exp3. In both cases, we found a decrease of complexity in the dynamics of phasic signals.

Table 2 reports on the results of Wilcoxon test with FDR post-hoc correction applied to SampEn values related to the four experimental protocols. SampEn estimates of resting sessions and stressful tasks were not statistically different for Exp1, Exp2, and Exp3. When we compared the Stroop Color and Word Test with the resting state (Exp4), we found significant p-values using the EDA signals (p-value < 0.001) and the tonic component (p-value <0.05). In both cases, entropy median values increased during the stressful task, as in ComEDA (see Table 1).

4. Discussion

We presented ComEDA, a dedicated novel methodological approach for the investigation of complex dynamics of EDA signals. The aim of ComEDA is to effectively estimate the complexity of the EDA signal to unveil changes in EDA response induced by different sources of sympathetic activation: physical effort and cognitive stress.

Table 2
Results of statistical tests applied to SampEn values extracted from EDA, tonic and phasic time series in the four experimental protocols used in this study (Exp1, Exp2, Exp3, Exp4), in terms of p-values obtained from the application of Wilcoxon non-parametric test, and corrected through FDR procedure. For each test, the corresponding trend of SampEn median value is shown by using the symbols ↓ and ↑, which indicate a decrease and an increase of SampEn median values during the stressful task with respect to the preceding rest, respectively. *n.s.* stands for not-significant p-value (p-value > 0.05).

SampEn	EDA		Tonic		Phasic	
	p-value	Trend	p-value	Trend	p-value	Trend
Exp1 (rest vs. hg)	n.s.		n.s.		n.s.	
Exp2 (rest vs. resp)	n.s.		n.s.		n.s.	
Exp3 (rest vs. mc)	n.s.		n.s.		n.s.	
Exp4 (rest vs. stroop)	0.0024	↑	0.0014	↑	n.s.	

Previous studies in the literature endeavored to define the regions of the brain and body involved in different sympathetic arousal phenomena, hypothesizing descending patterns (from the brain to the skin) and ascending ways (from viscera to brain) according to different neurobehavioural processes [62]. The main difference was hypothesized between the regulatory mechanisms underlying physical and psychological stressors [63]. A predominant bottom-up hierarchical scheme was highlighted in response to physical efforts, when the information was supposed to move from peripheral organs to brainstem and hypothalamus, mainly mediated by the activity of subcortical regions. On the other hand, during cognitive tasks, i.e. mental stressors, higher cortical levels, e.g. prefrontal cortex, were demonstrated to be involved in a top-down regulation pattern [64]. Carter et al. suggested that such complex autonomic dynamics during mental stress can be related to a disassociation between muscle sympathetic nerve activity (MSNA) and vascular response [26].

In this study, we propose the first comprehensive analysis of the complexity of EDA signals dynamics during the two main categories of stress, i.e. mental and physical, that are likely to be associated to different neural pathways. To this aim, we explored the complexity of dynamics of EDA signals, as well as of its two principal constituents, i.e. the phasic and tonic components, extracted through the cvxEDA method [17]. We purposely designed the ComEDA algorithm, which accepts as input an ultra-short segment of EDA signals and reconstructs the trajectory of the related attractor in the phase-space by using its optimal values of embedding dimension and time-delay. In this study we applied the ComEDA algorithm on the EDA as a whole and on the two components of which it is made up, i.e. tonic and phasic. ComEDA is able to provide a quantifier of the spatial complexity of the attractor

in the range [0,1], computing the normalized quadratic Rényi entropy of the PDF of the angular distances between the attractor points.

We first tested the proposed algorithm using a synthetic dataset consisting of 200 realizations of WGN noise and 200 realizations of 1/f series. Results point out that ComEDA is able to discriminate the complexity degree of two different processes, also in the case of ultra-short series and even using windows of only 50 samples. The performance of our algorithm indicates an increasing relevance if compared with different entropy algorithms in the literature which need a multiscale approach and, consequently, a much higher number of samples to be able to give appropriate information on the level of complexity [37].

Four experimental protocols were investigated: in experiments Exp1 and Exp2, we compared the resting sessions with two different physical efforts (submaximal hand-grip *hg*, and forced maximal exhalation *resp*, respectively), in Exp3 and Exp4 we compared the resting states with two mental efforts, i.e., mental computation, *mc*, and Stroop Color and Word Test, respectively.

Table 1 shows all the statistical results obtained through ComEDA algorithm. Some values of complexity of tonic and phasic components compared to the resting state in some stressful tasks are not statistically significant. On the other hand, we obtained significant and sound results about the complexity calculated from the EDA signals. Specifically, as it can be noticed from Table 1, the complexity of EDA decreases during a sympathetic activation induced by physical stress, i.e., *hg* and *resp* in Exp1 and Exp2, respectively, while it increases during mental efforts, i.e., *mc* and *stroop* in Exp3 and Exp4, respectively. This relevant result might be in support of the hypothesis of the main difference between the physiological patterns that regulate the sympathetic activation during physical and mental efforts [63]. Indeed, two main opposite different patterns of complexity changes have been found in EDA signals during physical compared to mental effort. Accordingly, we could hypothesize that a decrease of complexity of EDA dynamics can be associated to a predominant bottom-up hierarchical scheme, while an increase of it could be referred to a top-down regulation pattern. It is worthwhile noting that this difference of complexity is evident and consistent when the ComEDA algorithm is applied to the EDA signals, pointing out two clear opposite trends. Also investigating tonic complex dynamics it is possible to discern similar trends, although in some cases, e.g., *mc* in Exp3, results are not statistically significant.

We compared the performance of ComEDA with a previously defined entropy algorithm, SampEn [19,46]. For each time series, we computed SampEn starting from a phase space reconstructed in the same way as ComEDA. The results obtained with SampEn did not present statistically significant differences in most of the examined conditions (see Table 2). In fact, for Exp1, Exp2, and Exp3 we were not able to distinguish the experimental sessions with any of the time series taken into account (EDA, and tonic and phasic components). We showed a statistically significant difference only in the case of Exp4, for EDA and tonic component, where we reported for SampEn median values the same trends already found in ComEDA (see Table 2). Our findings suggest that the ComEDA approach improves on the state of the art on complexity assessment of EDA dynamics.

These promising results were obtained applying chaos theory to ultra-short time segments (one or two minutes) of EDA, tonic, and phasic signals, setting a sampling frequency of 4 Hz. These specifications make our algorithm easier to be implemented on wearable acquisition systems, which can allow a long-term monitoring of subjects during daily activities. In this way, continuous monitoring of subjects could be useful for the diagnosis of atypical sympathetic response to stressful situations, which can easily lead to anxiety and phobias.

Future works will be addressed towards the use of our approach to groups of healthy and pathological subjects monitored in a naturalistic environment. An interesting application of our algorithm could be to investigate complexity changes during emotional elicitation. Emotional arousal is characterized by two 'waves' of autonomic response [65]: the adrenomedullary activation (present also in response to other stressors), and the adrenocortical response. During emotional arousal, adrenomedullary and adrenocortical hormones interact with the amygdala to modulate memory-storage processes in other brain regions [66, 67]. Memories indeed play a fundamental role in the processing of emotional stimuli, which is not present during the reaction to purely physical stimuli. Furthermore, future endeavors will be directed at studying ComEDA performance according to the signal window size.

Declaration of competing interest

The authors declare that they have no known competing financial interests or personal relationships that could have appeared to influence the work reported in this paper.

Acknowledgments

The research leading to these results has received partial funding from European Union Horizon 2020 Programme under grant agreement n 824153 of the project "POTION-Promoting Social Interaction through Emotional Body Odours" and from the Italian Ministry of Education and Research (MIUR) in the framework of the CrossLab project (Departments of Excellence).

Appendix

The Matlab code for ComEDA index estimation is publicly available online at https://github.com/NardelliM/ComEDA.

References

[1] D.C. Fowles, M.J. Christie, R. Edelberg, W.W. Grings, D.T. Lykken, P.H. Venables, Publication recommendations for electrodermal measurements, Psychophysiology 18 (3) (1981) 232–239.
[2] R. Edelberg, Electrical activity of the skin: Its measurement and uses in psychophysiology, Handb. Psychophysiol. (1972) 367–418.
[3] W. Boucsein, Electrodermal Activity, Springer Science & Business Media, 2012.
[4] D. Leiner, A. Fahr, H. Früh, EDA positive change: A simple algorithm for electrodermal activity to measure general audience arousal during media exposure, Commun. Methods Meas. 6 (4) (2012) 237–250.
[5] J. Andreassi, Electrodermal activity (EDA) and behavior. Psychophysiology: Human behavior & physiological response (191–202), 2000.
[6] J.T. Cacioppo, L.G. Tassinary, G. Berntson, Handbook of Psychophysiology, Cambridge University Press, 2007.
[7] A.L. Goldberger, D.R. Rigney, B.J. West, Chaos and fractals in human physiology, Sci. Am. 262 (2) (1990) 42–49.
[8] J.P. Higgins, Nonlinear systems in medicine, Yale J. Biol. Med. 75 (5–6) (2002) 247.
[9] G. Sugihara, W. Allan, D. Sobel, K.D. Allan, Nonlinear control of heart rate variability in human infants, Proc. Natl. Acad. Sci. 93 (6) (1996) 2608–2613.
[10] A. Porta, S. Guzzetti, R. Furlan, T. Gnecchi-Ruscone, N. Montano, A. Malliani, Complexity and nonlinearity in short-term heart period variability: comparison of methods based on local nonlinear prediction, IEEE Trans. Biomed. Eng. 54 (1) (2006) 94–106.
[11] U.R. Acharya, K.P. Joseph, N. Kannathal, C.M. Lim, J.S. Suri, Heart rate variability: a review, Med. Biol. Eng. Comput. 44 (12) (2006) 1031–1051.
[12] M. Nardelli, A. Lanata, G. Bertschy, E.P. Scilingo, G. Valenza, Heartbeat complexity modulation in bipolar disorder during daytime and nighttime, Sci. Rep. 7 (1) (2017) 1–11.
[13] M. Nardelli, A. Greco, J. Bolea, G. Valenza, E.P. Scilingo, R. Bailón, Reliability of lagged poincaré plot parameters in ultrashort heart rate variability series: Application on affective sounds, IEEE J. Biomed. Health Inf. 22 (3) (2017) 741–749.
[14] H. Young, D. Benton, We should be using nonlinear indices when relating heart-rate dynamics to cognition and mood, Sci. Rep. 5 (1) (2015) 1–16.
[15] C. Collet, C. Petit, A. Priez, A. Dittmar, Stroop color–word test, arousal, electrodermal activity and performance in a critical driving situation, Biol. Psychol. 69 (2) (2005) 195–203.
[16] M. Benedek, C. Kaernbach, A continuous measure of phasic electrodermal activity, J. Neurosci. Methods 190 (1) (2010) 80–91.
[17] A. Greco, G. Valenza, A. Lanata, E.P. Scilingo, L. Citi, cvxEDA: A convex optimization approach to electrodermal activity processing, IEEE Trans. Biomed. Eng. 63 (4) (2015) 797–804.

[18] S.M. Pincus, Approximate entropy as a measure of system complexity, Proc. Natl. Acad. Sci. 88 (6) (1991) 2297–2301.
[19] J.S. Richman, J.R. Moorman, Physiological time-series analysis using approximate entropy and sample entropy, Am. J. Physiol.-Heart Circ. Physiol. 278 (6) (2000) H2039–H2049.
[20] Z. Visnovcova, M. Mestanik, M. Gala, A. Mestanikova, I. Tonhajzerova, The complexity of electrodermal activity is altered in mental cognitive stressors, Comput. Biol. Med. 79 (2016) 123–129.
[21] M. Svetlak, P. Bob, M. Cernik, M. Kukleta, Electrodermal complexity during the stroop colour word test, Auton. Neurosci. 152 (1–2) (2010) 101–107.
[22] A.L. Mark, R.G. Victor, C. Nerhed, B.G. Wallin, Microneurographic studies of the mechanisms of sympathetic nerve responses to static exercise in humans, Circ. Res. 57 (3) (1985) 461–469.
[23] S.E. Nielsen, M. Mather, Comparison of two isometric handgrip protocols on sympathetic arousal in women, Physiol. Behav. 142 (2015) 5–13.
[24] Y. Kira, T. Ogura, S. Aramaki, T. Kubo, T. Hayasida, Y. Hirasawa, Sympathetic skin response evoked by respiratory stimulation as a measure of sympathetic function, Clin. Neurophysiol. 112 (5) (2001) 861–865.
[25] E. Anderson, C. Sinkey, A. Mark, Mental stress increases sympathetic nerve activity during sustained baroreceptor stimulation in humans, Hypertension 17 (4_supplement) (1991) III43.
[26] J.R. Carter, C.A. Ray, Sympathetic neural responses to mental stress: responders, nonresponders and sex differences, Am. J. Physiol.-Heart Circ. Physiol. 296 (3) (2009) H847–H853.
[27] M. Fechir, M. Gamer, I. Blasius, T. Bauermann, M. Breimhorst, P. Schlindwein, T. Schlereth, F. Birklein, Functional imaging of sympathetic activation during mental stress, Neuroimage 50 (2) (2010) 847–854.
[28] M.Z. Poh, N.C. Swenson, R.W. Picard, A wearable sensor for unobtrusive, long-term assessment of electrodermal activity, IEEE Trans. Biomed. Eng. 57 (5) (2010) 1243–1252.
[29] H.F. Posada-Quintero, J.P. Florian, A.D. Orjuela-Cañón, T. Aljama-Corrales, S. Charleston-Villalobos, K.H. Chon, Power spectral density analysis of electrodermal activity for sympathetic function assessment, Ann. Biomed. Eng. 44 (10) (2016) 3124–3135.
[30] R.P. Dum, D.J. Levinthal, P.L. Strick, The mind–body problem: Circuits that link the cerebral cortex to the adrenal medulla, Proc. Natl. Acad. Sci. 116 (52) (2019) 26321–26328.
[31] K. Dedovic, A. Duchesne, J. Andrews, V. Engert, J.C. Pruessner, The brain and the stress axis: the neural correlates of cortisol regulation in response to stress, Neuroimage 47 (3) (2009) 864–871.
[32] J.P. Herman, W.E. Cullinan, Neurocircuitry of stress: central control of the hypothalamo–pituitary–adrenocortical axis, Trends Neurosci. 20 (2) (1997) 78–84.
[33] K. Buller, C. Dayas, T. Day, Descending pathways from the paraventricular nucleus contribute to the recruitment of brainstem nuclei following a systemic immune challenge, Neuroscience 118 (1) (2003) 189–203.
[34] H. Sequeira, J.C. Roy, Cortical and hypothalamo-limbic control of electrodermal responses, in: Progress in Electrodermal Research, Springer, 1993, pp. 93–114.
[35] M. Mischi, C. Chen, T. Ignatenko, H. de Lau, B. Ding, S.G. Oei, C. Rabotti, Dedicated entropy measures for early assessment of pregnancy progression from single-channel electrohysterography, IEEE Trans. Biomed. Eng. 65 (4) (2017) 875–884.
[36] J.S. Richman, D.E. Lake, J.R. Moorman, Sample entropy, Methods Enzymol. 384 (2004) 172–184.
[37] M. Costa, A. Goldberger, C.K. Peng, Multiscale entropy to distinguish physiologic and synthetic RR time series, in: Computers in Cardiology, IEEE, 2002, pp. 137–140.
[38] M.U. Ahmed, D.P. Mandic, Multivariate multiscale entropy: A tool for complexity analysis of multichannel data, Phys. Rev. E 84 (6) (2011) 061918.
[39] M. Nardelli, E.P. Scilingo, G. Valenza, Multichannel Complexity Index (MCI) for a multi-organ physiological complexity assessment, Physica A 530 (2019) 121543.
[40] D.R. Seals, R.M. Enoka, Sympathetic activation is associated with increases in EMG during fatiguing exercise, J. Appl. Physiol. 66 (1) (1989) 88–95.
[41] M. Al'Absi, S. Bongard, T. Buchanan, G.A. Pincomb, J. Licinio, W.R. Lovallo, Cardiovascular and neuroendocrine adjustment to public speaking and mental arithmetic stressors, Psychophysiology 34 (3) (1997) 266–275.
[42] Y. Hoshikawa, Y. Yamamoto, Effects of stroop color-word conflict test on the autonomic nervous system responses, Am. J. Physiol.-Heart Circ. Physiol. 272 (3) (1997) H1113–H1121.
[43] F. Scarpina, S. Tagini, The stroop color and word test, Front. Psychol. 8 (2017) 557.
[44] J.R. Stroop, Studies of interference in serial verbal reactions, J. Exp. Psychol. 18 (6) (1935) 643.
[45] A. Ishchenko, P. Shev'ev, Automated complex for multiparameter analysis of the galvanic skin response signal, Biomed. Eng. 23 (3) (1989) 113–117.
[46] D.E. Lake, J.S. Richman, M.P. Griffin, J.R. Moorman, Sample entropy analysis of neonatal heart rate variability, Am. J. Physiol.-Regul. Integr. Comp. Physiol. 283 (3) (2002) R789–R797.
[47] F. Takens, Detecting strange attractors in turbulence, in: Dynamical Systems and Turbulence, Warwick 1980, Springer, 1981, pp. 366–381.
[48] H. Abarbanel, Analysis of Observed Chaotic Data, Springer Science & Business Media, 2012.
[49] H. Kim, R. Eykholt, J. Salas, Nonlinear dynamics, delay times, and embedding windows, Physica D 127 (1–2) (1999) 48–60.
[50] P. Li, C. Liu, K. Li, D. Zheng, C. Liu, Y. Hou, Assessing the complexity of short-term heartbeat interval series by distribution entropy, Med. Biol. Eng. Comput. 53 (1) (2015) 77–87.
[51] C. Karmakar, R.K. Udhayakumar, P. Li, S. Venkatesh, M. Palaniswami, Stability, consistency and performance of distribution entropy in analysing short length heart rate variability (HRV) signal, Front. Physiol. 8 (2017) 720.
[52] Z.I. Botev, J.F. Grotowski, D.P. Kroese, et al., Kernel density estimation via diffusion, Ann. Statist. 38 (5) (2010) 2916–2957.
[53] H.A. Sturges, The choice of a class interval, J. Amer. Statist. Assoc. 21 (153) (1926) 65–66.
[54] A. Rényi, et al., On measures of entropy and information, in: Proceedings of the Fourth Berkeley Symposium on Mathematical Statistics and Probability, Volume 1: Contributions to the Theory of Statistics, The Regents of the University of California, 1961.
[55] P. Castiglioni, M. Di Rienzo, How the threshold "r" influences approximate entropy analysis of heart-rate variability, in: 2008 Computers in Cardiology, IEEE, 2008, pp. 561–564.
[56] W. Chen, Z. Wang, H. Xie, W. Yu, Characterization of surface EMG signal based on fuzzy entropy, IEEE Trans. Neural Syst. Rehabil. Eng. 15 (2) (2007) 266–272.
[57] P.E. McKnight, J. Najab, Mann-Whitney U test, Corsini Encycl. Psychol. (2010) 1.
[58] N.M. Razali, Y.B. Wah, et al., Power comparisons of shapiro-wilk, kolmogorov-smirnov, lilliefors and anderson-darling tests, J. Stat. Model. Anal. 2 (1) (2011) 21–33.
[59] Y. Benjamini, A.M. Krieger, D. Yekutieli, Adaptive linear step-up procedures that control the false discovery rate, Biometrika 93 (3) (2006) 491–507.
[60] R.F. Woolson, Wilcoxon signed-rank test, Wiley Encycl. Clin. Trials (2007) 1–3.
[61] J.L. Hintze, R.D. Nelson, Violin plots: a box plot-density trace synergism, Amer. Statist. 52 (2) (1998) 181–184.
[62] G.G. Berntson, J.T. Cacioppo, M. Sarter, Bottom-up: Implications for neurobehavioral models of anxiety and autonomic regulation, 2003.
[63] I. Papousek, G. Schulter, E. Premsberger, Dissociated autonomic regulation during stress and physical complaints, J. Psychosom. Res. 52 (4) (2002) 257–266.
[64] P. Sawchenko, H. Li, A. Ericsson, Circuits and mechanisms governing hypothalamic responses to stress: a tale of two paradigms, Prog. Brain Res. 122 (2000) 61–80.
[65] L. Cahill, J.L. McGaugh, Mechanisms of emotional arousal and lasting declarative memory, Trends Neurosci. 21 (7) (1998) 294–299.
[66] B. Roozendaal, O. Carmi, J.L. McGaugh, Adrenocortical suppression blocks the memory-enhancing effects of amphetamine and epinephrine, Proc. Natl. Acad. Sci. 93 (4) (1996) 1429–1433.
[67] B. Roozendaal, A. Barsegyan, S. Lee, Adrenal stress hormones, amygdala activation, and memory for emotionally arousing experiences, Prog. Brain Res. 167 (2007) 79–97.